(NASA-CR-162351) WIND TUNNEL INVESTIGATION OF THE FREE-WING/FREE TRIMMER CONCEPT Status Report, Jan. - Oct. 1979 (Naval Academy) 59 p HC A04/MF A01 CSCL 01C

N79-33216

Unclas
G3/08 35902

STATUS REPORT OF WIND TUNNEL INVESTIGATION OF THE FREE-WING/FREE-TRIMMER CONCEPT

PRINCIPAL INVESTIGATOR - DORAL R. SANDLIN
PERIOD COVERED - JAN 1979 - OCTOBER 1979
GRANTEE - DFRC (NASA), EDWARDS AFB, CALIFORNIA
GRANT NUMBER - NSG 4020

ABSTRACT

Previous studies have indicated that several benefits, most importantly that of gust alleviation, can be realized by aircraft employing an unconventional wing, free to pivot about a spanwise axis forward of the aerodynamic center. To obtain reasonably high lift coefficients, a secondary surface, also free to pivot, has been attached to the wing in either a forward or aft position with respect to the wing pivot. This is known as a free-wing / free-trimmer concept, developed by NASA.

At present, only an analytical model and limited flight tests of a radio-controlled model have been used to investigate this concept. This paper describes a preliminary wind tunnel analysis of a free-wing / free-trimmer model, employing an aft-mounted, wing-tip trimmer. It provides an introduction and background for future wind tunnel studies.

Relatively little data was obtained in support of the analytical model, due to problems encountered during testing. An analysis of these difficulties and their solutions is presented, with recommendations toward future testing.

The conclusions arrived at in this investigation are ;

(1) The free-wing / free-trimmer configuration is a viable concept, and exhibited both static and dynamic stability for a trimmer pivot at the 10 percent chord position. More testing is needed however, for a 19 percent of chord pivot, and to determine the optimum direction for the trimmer camber with respect to the wing camber.

(2) Unless properly controlled, friction in the mounting system and instrumentation can significantly affect the panel response. Reduction of this effect can be realized by increasing the size of the model and / or the tunnel velocity.

(3) For the configurations tested, the control was far too sensitive, giving the full range of wing angle-of-attack for trimmer flap displacements of only a few degrees. To reduce this sensitivity, the wing pivot axis should be moved forward.

(4) Further testing should include an analysis of the maximum lift coefficient obtainable with a trailing edge flap on the wing, and the effect of configuration changes on the maximum lift.

NOMENCLATURE

LOWER CASE

a	lift-curve slope
b	wing span
c	chord
g	gravitational constant
h	distance from wing pivot to trimmer pivot, distance to a point, perpendicular from trailing vortex
l	distance from pivot to center of gravity
m	mass
mfd	millifarad
t	time
x	distance from pivot to aerodynamic center, distance to a point, perpendicular to bound vortex
y	distance perpendicular to trailing vortex to a point on the trimmer

UPPER CASE

AR	aspect ratio
C_l	wing lift coefficient
C_m	wing pitching moment coefficient
C_{m_δ}	partial derivitive of the pitching moment coefficient with respect to control surface deflection
F	frictional torque
I_y	moment of inertia about about pivot

M_p	aerodynamic pitching moment about pivot axis
Rn	Reynolds number
S	wing area
V	free-stream velocity

GREEK

α	angle-of-attack
α, β	angle formed by a vortex filiment and a line from the the vortex end to a point
Γ	circulation
δ	flap or control deflection, damping ratio
θ	angle of displacement
ν	kinematic viscousity
ρ	density
ω	upwash velocity
Ω	ohms

SUBSCRIPTS

f	relating to flap
l_0	zero lift value
0	infinite aspect ratio
t	relating to the trimmer
w	relating to the wing

OTHER

$\dot{}$	first derivitive with respect to time
$\ddot{}$	second derivitive with respect to time
$\|_\delta$	corresponding to a control deflection of δ

TABLE OF CONTENTS

LIST OF FIGURES

LIST OF TABLES

INTRODUCTION

BACKGROUND

Conventional low-wing loading aircraft have long suffered from poor ride quality in turbulence. As a result, light aircraft have not had the acceptance as a practical means of transportation. This problem is compounded by the fact that light aircraft spend a major portion of their flight time at lower altitudes, where turbulence is likely to be encountered.

The ride quality can be improved by an increase in wing loading, but this results in a lower minimum flying speed, and increased takeoff and landing distances. Since a main advantage of light aircraft is their ability to operate out of shorter fields, this is not a practical solution.

Methods of reducing gust loading, without an increase in wing loading may be conveniently classified according to the gust alleviation system employed:

(1) Pitching the entire aircraft by use of the elevators to maintain a constant angle-of-attack.

(2) Vary the incidence of the wing to maintain a constant angle-of-attack.

(3) Operation of flaps, spoilers, or deflectors to offset the lift increments on the wing.

A very effective approach to gust alleviation is the free-wing concept, which may be broadly classified in category (2). However, it's gust alleviation performance is considerably superior to that achievable by direct mechanical control of the wing incidence angle. The major disadvantage of the free-wing is the relatively low maximum lift coefficient obtainable.

An extension to the free-wing concept is the NASA-conceived free-wing / free-trimmer, which provides sufficient trimming power to allow the use of high-lift trailing edge flaps on the wing.

FREE-WING CONCEPT

The original concept of the free-wing was disclosed in U.S. Patent No. 2347230 issued to Daniel R. Zuck in 1944. In 1945, he built a small prototype which was never successfully flown.

As conceived by Zuck, the two wing panels of a free-wing aircraft are free to rotate independently about a spanwise axis, and are controlled by means of a trailing-edge flap. The panels are subject only to aerodynamic pitching moments and unrestricted by mechanical constraints. Static pitching stability is provided by pivoting the panels forward of the aerodynamic center, and equilibrium is obtained by a balance of moments created by the trailing-edge control surface and lift and drag forces.

The gust alleviation feature of this concept is that the wing tends to maintain a prescribed lift coefficient when subjected to a change in flow direction. While all aircraft have this tendency, the greatly reduced pitching moment of inertia of the free-wing panels results in a more rapid response to gust impulses.

PREVIOUS FREE-WING WORK

The first analytical study[1] to predict the dynamic longitudinal response of a free-wing aircraft allowed independent motion of the left and right panels. The result of this study was the development of the complete set of equations of motion for an aircraft employing the free-wing concept, and the evaluation of three hypothetical subsonic aircraft, ranging in gross weight from 3000 to 50,000 pounds.

The lateral and longitudinal equations of motion were linearized about straight and level conditions, and the aircraft response to gust and control inputs determined by examining the characteristic roots of the motion equations.

The following conclusions were drawn from this work:

(1) Most atmospheric effects were greatly reduced, particularly the root-mean-square load factor and rolling disturbances. The rms fuselage pitch rate was significantly increased in comparison with equivalent fixed-wing aircraft.

(2) All stick-fixed modes of motion were stable, except for the spiral mode.

(3) The lateral-directional handling qualities were unsatisfactory because of the combination of low roll damping and spiral divergence.

(4) Artifical stability augmentation, in the form of a simple roll damper, provided excellent lateral control and turbulence penetration characteristics.

From the results of this study, a second study(2) was performed to provide a realistic and comprehensive analysis of the practical aspects of utilizing the free-wing concept for light aircraft. This study was basically analytical in nature, but was supported by limited wind tunnel tests of pitch and yaw models.

The conclusions from this report were:

(1) The free-wing concept can be applied to unsopisticated low wing loading aircraft to provide ride quality equal or superior to aircraft with much higher wing loading.

(2) For free-wing aircraft without differential wing panel freedom, all pertinent handling qualities, and certification criteria can be met without recourse to stability augmentation.

(3) Differential pitch freedom between the left and right wing panels should not be permitted for aircraft in this class; although the serious lateral deficiencies accompanying such freedom can be corrected with passive mechanical devices.

(4) Leading edge slats are necessary for takeoff and landing to compensate for the low maximum lift coefficient inherent in free-wing aircraft.

(5) The free-wing panels should be balanced about the spanwise hinge axis with leading edge slats retracted; thus a ballast weight penalty is incurred.

FREE-WING / FREE-TRIMMER CONCEPT

The free-wing / free-trimmer concept is a NASA-conceived extension to the free-wing to provide sufficient trimming power for the use of high-lift trailing-edge flaps. The wing is controlled by a pitching moment about the hinge axis by aerodynamic lift on a small trimmer attached to the wing. This trimmer is located either fore or aft of the wing pivot, and is also allowed to pivot freely about a spanwise axis forward of it's aerodynamic center. Pitch control of the entire assembly is provided by a trailing edge flap on the trimming surface.

PREVIOUS ANALYTICAL WORK

An analytical study[3] of the free-wing / free-trimmer concept as applied to small aircraft was performed by Battelle Columbus Laboratories under contract to NASA. This study was limited to stick-fixed longitudinal motion, gust alleviation characteristics, and an assessment of the response to symmetric vertical turbulence and control surface step inputs.

A preliminary design of several conceptual free-wing/free-trimmer aircraft was performed to provide representative dimensional and mass parameters for the mathematical models. Both fore and aft trimmers were considered, with varying moment arms, and the left and right wing panels were restricted to symmetric deflection only.

The equations of motion for the longitudinal direction were developed, resulting in thirteen equations and variables representing the five degrees of freedom system. A linear analysis was performed of the gust alleviation characteristics and handling qualities as indicated by the characteristic roots associated with the stick-fixed longitudinal modes.

The following conclusions were drawn from this investigation:

(1) For the trimmer to wing area ratio considered (1/6), the most promising configuration employs aft-mounted wing tip trimmer surfaces with a one-chord moment arm.

(2) For vertical gust alleviation, forward trimmers are inferior to aft-mounted surfaces

(3) Mass balancing of the trimmer surface about it's hinge axis is vital to the characteristic mode stability.

(4) Longitudinal displacement of the fuselage center of gravity appears to be more significant for free-wing / free-trimmer configurations than for pure free-wing aircraft

(5) Small variations in the wing assembly center of gravity (for a few percent of wing chord) have no significant effect on the in-flight characteristic modes.

(6) Forward trimmer configurations are more efficient from a weight standpoint than aft-mounted configurations.

PURPOSE OF THIS INVESTIGATION

The purpose of this work is to test a model, representative of the free-wing/free-trimmer, in the 3 by 4 foot wind tunnel belonging to the Aeronautical Engineering Department, California Polytechnic State University, San Luis Obispo. This report describes the problems encountered, attempts at correction and an analysis of possible methods of avoiding these difficulties.

The results of this study are intended to provide support of the analytical investigation performed for NASA Dryden Flight Research Center,[3] and as a background for future wind tunnel tests. Furthermore, an assessment of configuration changes on the static and dynamic characteristics of the free-wing/free-trimmer system is included.

SCOPE

The investigation described in this report is limited to control-fixed longitudinal motion of a free-wing/free-trimmer system in which the wing is pivoted at the 19 percent chord position. The trimmer was mounted aft of the wing pivot on the wing tip, at a distance of one wing chord from the wing pivot to the trimmer pivot.

The trimmer was also confined to longitudinal motion only, but two pivot locations were evaluated, these being at 10 percent and 19 percent of the trimmer chord. Flap sizes of 10, 20 and 30 percent of the trimmer chord were analized for their effect on the system, and due to the extreme sensitivity of the trimmer, a small trimmer was also tested.

In all cases the wing/trimmer system was mounted vertically in the tunnel to eliminate gravitational influences and provide a response more indicative of the aerodynamic moments associated with the configuration. When possible, geometric parameters were maintained consistant with those in the analytical study of the free-wing/free-trimmer concept. Since time was limited, as thorough as an investigation as possible was not conducted, and testing was limited to determining general characteristics and response of the system to configuration changes rather than the accumulation of data points.

PROCEDURE

CONSTRUCTION OF THE WING

The model of the wing used in the testing described in this report was constructed of solid wood with a chord of 5 and a span of 20 inches giving an AR of 4. Maximum thickness of the wing was 12 percent of the chord, and while the profile did not exactly correspond to a NASA 23012 section, it was sufficiently close that subsequent calculations were based on this profile data. It was desired to maintain geometric similarity with the analytical model in Reference 3, which used a wing aspect ratio 6, but since the above wing was already available, it was used in this investigation. An endplate was attached to one end of the model, and as a result testing was done with effectively a semispan model of a wing of an aspect ratio 8.

Booms were mounted on the root and the tip of the wing to allow for support of the trimmer, and mass balancing of the wing/trimmer configuration about the wing pivot. The booms were aligned with the wing chord so as to give a visual reference of wing angle-of-attack while in the wing tunnel.

CONSTRUCTION OF TRIMMER

The aft location of the trimmer in this investigation was selected since it was desired to instrument the trimmer so as to have an accurate and permanent record of it's angular variation with respect to the wing chord. Any instrumentation mounted in front of the wing would interfere with the flow over the wing, while for an aft location, the only influence on the system would be drag, which for a small range of angles-of-attack would act through the wing pivot, and thus contribute nothing to the moment about the pivot. The tip-mounted position was used to not only take advantage of the upwash due to tip vortices, but to conform to Configuration 1c in Reference 3.

The ratio of trimmer area to wing area is 1 to 6 and the ratio of their respective aspect ratios is 1 to 4, which results in a trimmer of chord 2.9 and a span of 5.8 inches. For ease of construction and low weight, the trimmer was made from solid balsa wood with a NACA 23012 section profile. The trimmer was mounted and supported to the tip boom by an eighth-inch shaft and two bearings located in the boom. The variation in pivot position was accomplished by holes in the trimmer at 10 and 19 percent chord in which the shaft could be slipped. Mass balancing was provided by a threaded rod attached to the support rod between the trimmer and boom, to reduce the effect on the trimmer of flow disturbances which would result from a weight directly in front of the trimmer.

MOUNTING SYSTEM

The initial plan for mounting the wing/trimmer model was to support it on a single 3/16 inch shaft extending through the wind tunnel floor, isolated from tunnel vibrations. This shaft in turn is supported by two bearings external to the wind tunnel, and since it rotates with the wing, the instrumentation for the wing is also external to the tunnel. This mounting system is shown by the photograph in Figure (3).

Since the wing was to be located outside of the influence of the tunnel wall boundary layer, the free length of the support shaft from bearing to model is about 4 inches. It was found that this length of shaft resulted in insufficient rigidity of the model in the wind tunnel. To correct this problem, a three-wire, Y-braced system was devised to support the upper end of the wing in the tunnel, since a shaft extending from the top of the tunnel would disturb the flow over the aft-mounted trimmer surface. The three wires were isolated from the tunnel vibrations by running them through the tunnel walls and attaching them to a rigid framework built around the test section. As shown in Figure (4) the lower mount was also attached to the support struc-

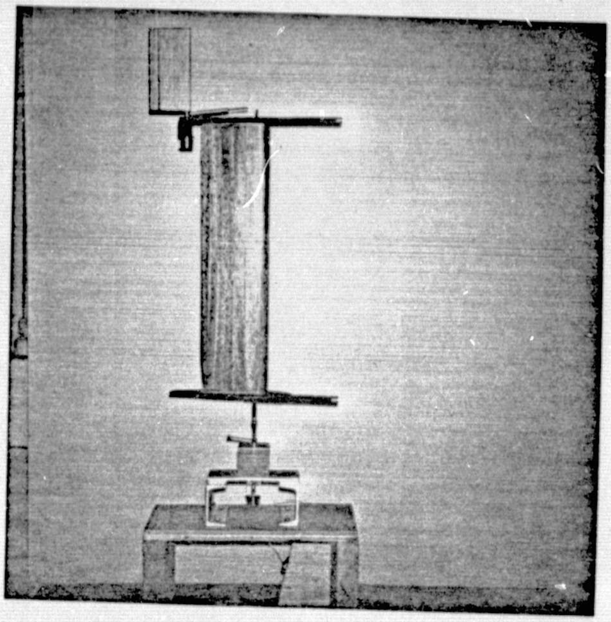

FIGURE 1: FREE-WING/FREE-TRIMMER MODEL AND LOWER MOUNT

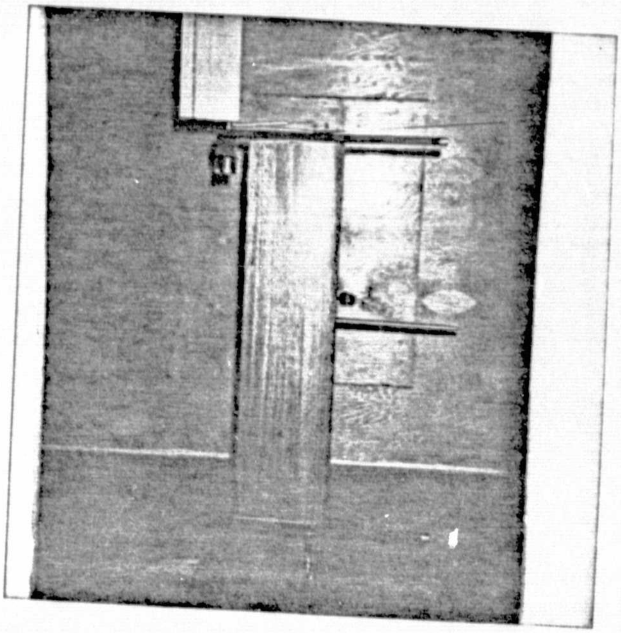

Side View

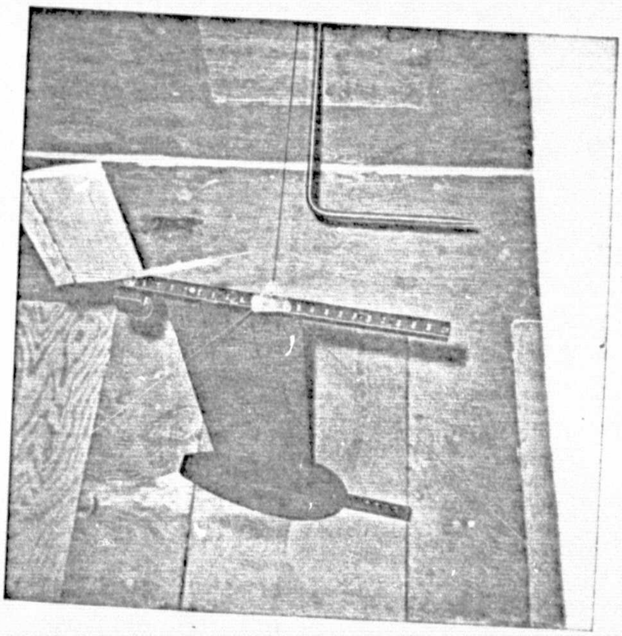

Top View

FIGURE 2: MODEL IN TEST SECTION OF TUNNEL

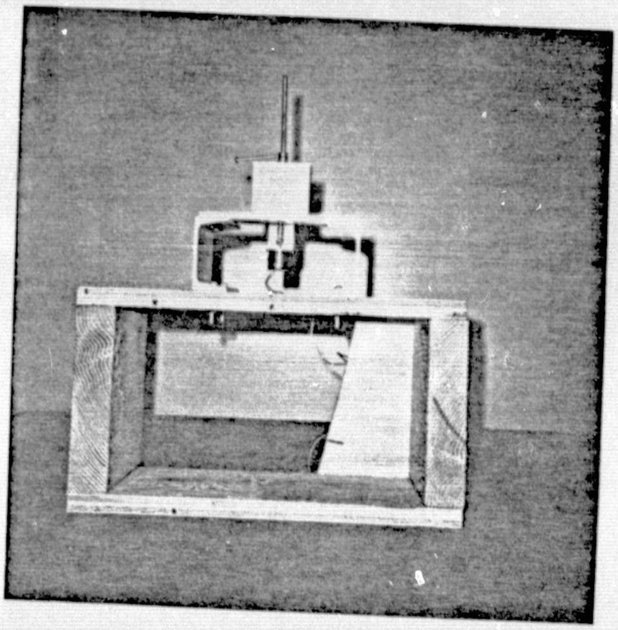

FIGURE 3: LOWER MOUNT/SUPPORT

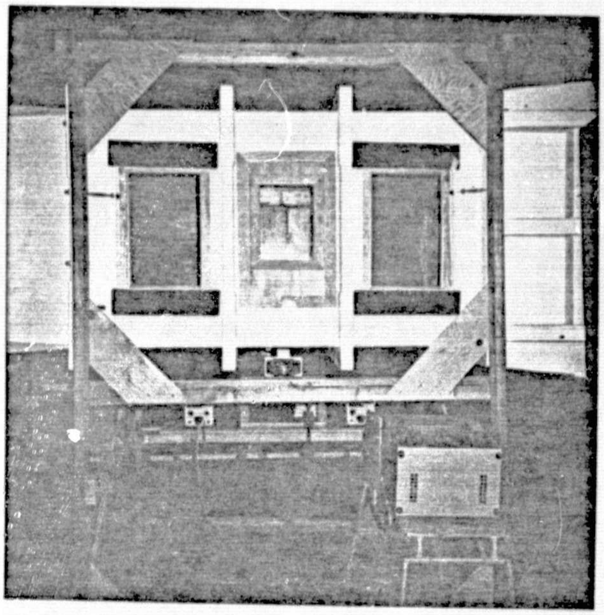

FIGURE 4: EXTERNAL SUPPORT STRUCTURE AND
WIND TUNNEL TEST SECTION

ture so that any vibrations induced in the framework from the floor would be picked up equally by the lower mount and upper wire supports. This system seemed to work well, since during testing, no vibrations could be felt in any of the mounting components.

INSTRUMENTATION

The method for obtaining a permanent record of the time response of a free-wing model described in NASA report CR-2046 was iniatially used in this investigation. This approach consists of monitering with a strip-chart recorder the variation in voltage across a 360 degree potentiometer connected to the pivot axis of the model.

For the free-wing/free-trimmer configuration, two potentiometers were used to record the angular changes in both the wing and the trimmer, and readout was to a dual-channel, strip-chart recorder. The location of the potentiometer are shown in Figures 1 and 3, and the circuit is illustrated schematically in Figure 5.

As testing of the free-wing/free-trimmer model progressed, it became apparent that frictional torque in the potentiometers was of sufficient magnitude to mask the trimmer response due to aerodynamic moments, and alter the wing response. As a result, the trimmer potentiometer was removed and the wing potentiometer replaced by a resolver of considerably less friction.

Since this resolver operates by changes in the electric field strength, it was necessary to incorporate a signal generator and half-wave rectifier as indicated in the circuit shown in Figure 6.

CALIBRATION AND COMPUTATION OF INERTIA PARAMETERS

The wing and trimmer potentiometers were calibrated with the strip-chart recorder so as to read 1 degree angular change for 1mm pen movement, and calibration runs are shown in Figure 7 for angles of $\pm$ 20 degrees. As indicated, the potentiometers were found to be linear over the range of $\pm$ 10 degrees with vary slight variations beyond that range.

For both the trimmer and wing circuits, the D.C. power supply was adjusted to give 40 V.D.C at 100 mA current. The potentiometer was then set so that 12.5 volts was indicated on the power supply meter, giving the initial zero potentiometer position. The gain and sensitivity of the recorder was then adjusted to give 1mm deflection per degree of rotation, and the pen positioned to zero on the recording paper.

With the calibrations completed, the moment of inertia of the wing and trimmer, and friction in the system was estimated. The wing/trimmer combination was supported by its axis, displaced, and allowed to oscillate, resulted in the trace shown in Figure 8. This system is a simple pendulum, in which the motion

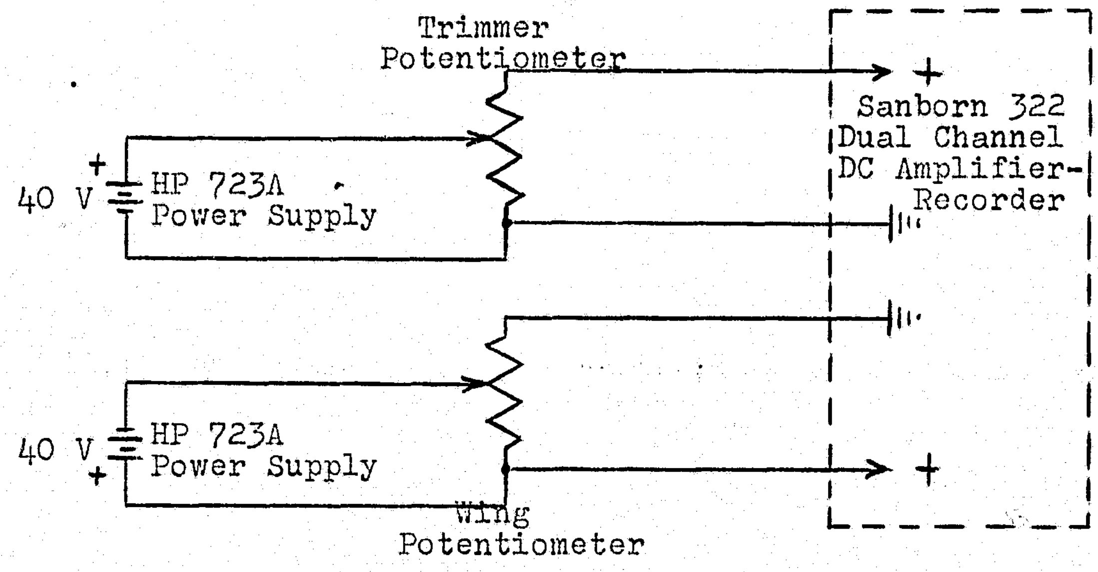

FIGURE 5 : SCHEMATIC DIAGRAM OF POTENTIOMETER CIRCUIT

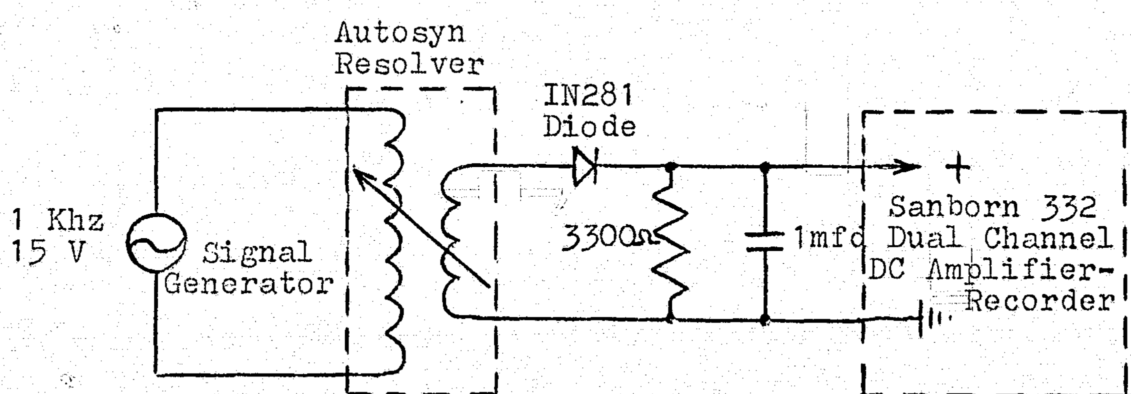

FIGURE 6 : SCHEMATIC DIAGRAM OF RESOLVER CIRCUIT

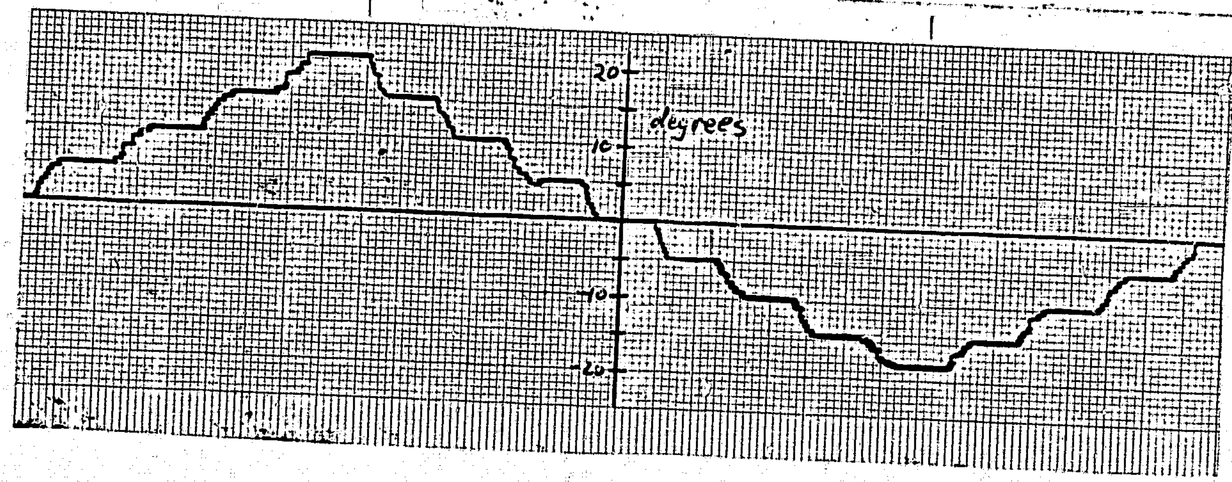

Wing Calibration

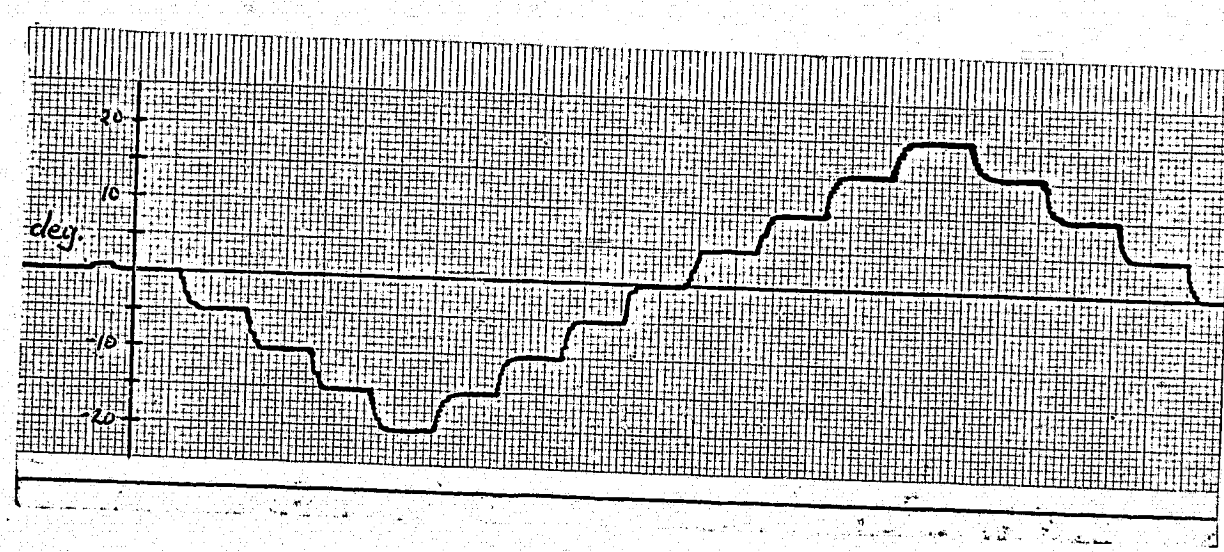

Trimmer Calibration

FIGURE 7: WING AND TRIMMER POTENTIOMETER CALIBRATIONS

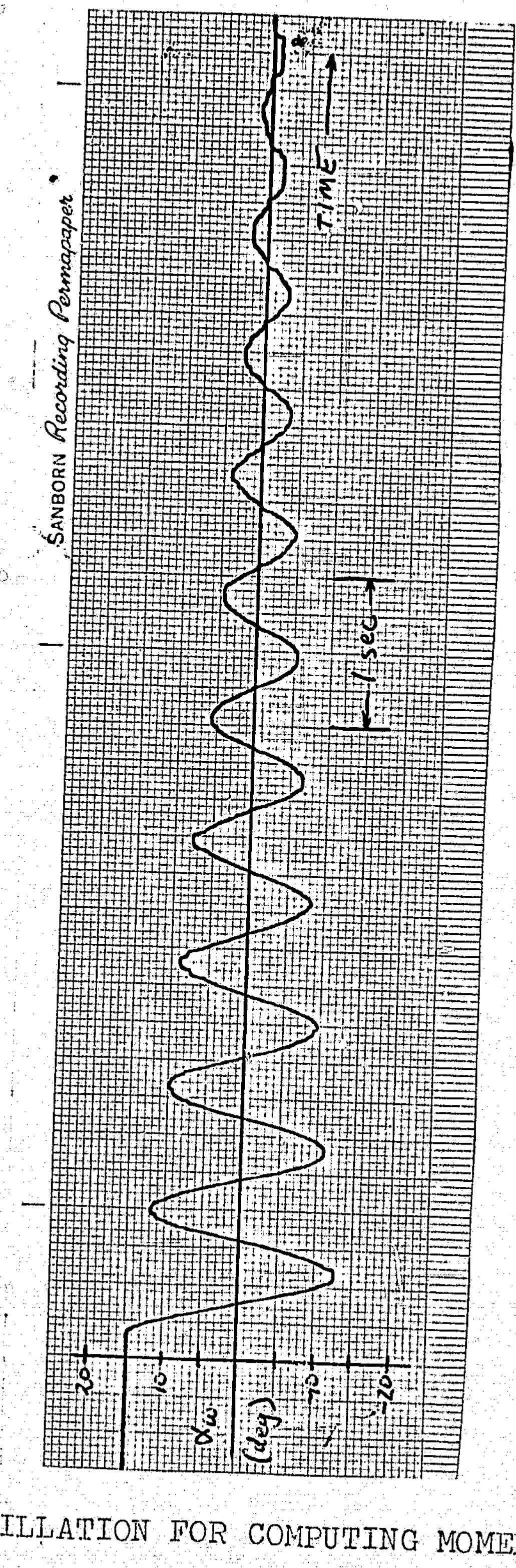

FIGURE 8: WING OSCILLATION FOR COMPUTING MOMENT OF INERTIA AND FRICTIONAL TORQUE

is governed by the expression:

$$I_y\ddot{\theta} + mgl\sin\theta + F\,\mathrm{sgn}\,\dot{\theta} = 0$$

The moment of inertia and frictional damping are then computed from the oscillation response by the relations:

$$I_y = mgl/w^2 \qquad \text{and} \qquad F = \delta\, mgl/4$$

where w is the frequency and δ is the amplitude decay per cycle. The contribution to the moment of inertia of adding the mass balancing weights is then computed analytically and added to that determined above to find the total wing/trimmer inertia about the wing pivot axis, and the results are shown in Table 1.

A similar analysis was performed to find the trimmer moments of inertia, however it was found that the inertia of the trimmer alone was too small to provide sufficient response. A weight was therefore added to the trimmer to increase the moment of inertia, the combination was oscillated, and then the inertia of the weight was subtracted from the results. The strip-chart recordings and computed results are shown in Figure 9 and Table 1 respectively.

When later in the testing program, the resolver was substituted in place of the potentiometer, a similar

TABLE 1: MOMENTS OF INERTIA

Description of item(s)	m (gr)	l (mm)	w (sec^{-1})	I_y of item (slug-in^2)	I_y corrected for weight (slug-in^2)
weight	17.9	70	10.83	.0111	-----
trimmer and weight 20% chord 19% pivot	32.4	47.6	11.42	.0123	-----
trimmer alone	14.5	---	-----	.0012	.0028
trimmer and weight 20% chord 10% pivot	32.4	50.8	11.63	.0127	-----
trimmer alone	14.5	---	-----	.0016	.0035
trimmer and weight 30% chord 19% pivot	31.0	49.3	11.42	.0122	-----
trimmer alone	13.1	---	-----	.0011	.0027
trimmer and weight 30% chord 10% pivot	31.0	52.3	11.42	.0129	-----
trimmer alone	13.1	---	-----	.0018	.0037
wing	855	34	7.616	.5234	.9901

TABLE 2: FRICTIONAL TORQUE

Description of item	m (gr)	l (mm)	δ	F (in-lbs)
trimmer potentiometer	17.9	70	.916	.299
wing potentiometer	855	34	.202	.128
resolver	822	18	.160	.0521

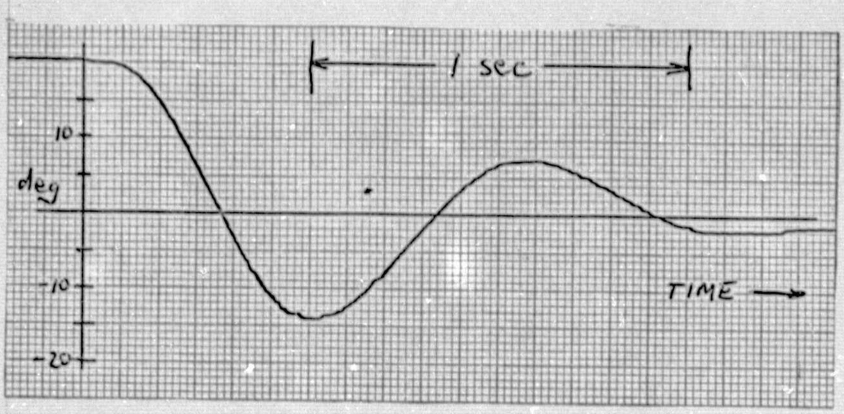

Weight oscillation alone

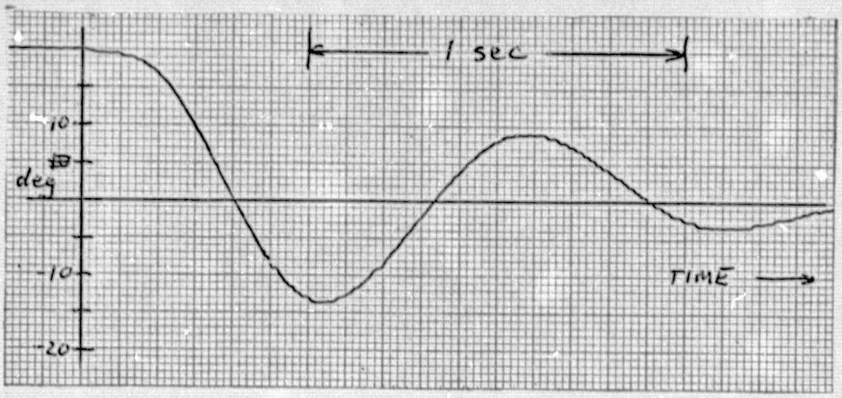

Weight and trimmer oscillation; 20% flap, 10% pivot

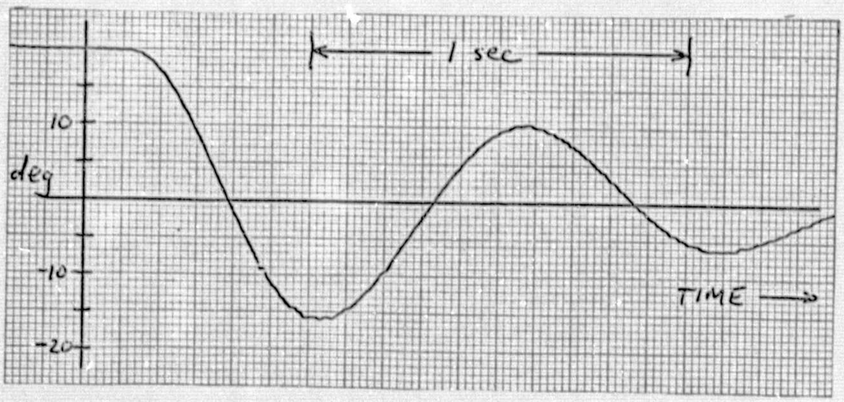

Weight and trimmer oscillation; 20% flap, 19% pivot

FIGURE 9: OSCILLATIONS FOR COMPUTING TRIMMER MOMENT OF INERTIA AND FRICTIONAL TORQUE

analysis was performed to compute its' friction, and the result is shown along with the pot friction in Table 2. A calibration test was performed, and the resolver was found to be linear in the range of ± 10 degrees with about one degree variation at ± 15 degrees. For these tests the signal generator was set at a frequency of 1-kHz, with an RMS voltage of 15, and the gain sensitivity was again adjusted to give one degree per mm deflection reading on the strip recorder.

TESTING PROCEDURE

At the start of this investigation, a testing procedure was established to provide a systematic and comprehensive analysis of the free-wing/free-trimmer concept. Simply stated, this procedure consists of determining the trim conditions for various control deflections, then disturbing the system positively and negatively and recording the time response to these disturbances.

Unfortunately, a large number of problems were encountered throughout testing, and this outlined procedure could not be adhered to. Furthermore, these difficulties and the limited time available, made a systematic approach to solving these problems impossible to follow.

Initially, a trimmer with a 10 percent chord flap surface, pivoted at the 19 percent chord position, was constructed and tested in the wind tunnel. Only the wing potentiometer was connected, but not calibrated at this time, so the actual angle-of-attack of the wing and trimmer could not be determined, although the wing response could be monitored. The lower mount was isolated from the tunnel, but the support wires were attached to the tunnel walls.

A stable system was observed for small flap deflection angles, however for flap angles greater than about ± 5 degrees, an oscillation occured in the trimmer surface, which increased in magnitude as the deflection angle increased. As a result of the trimmer motion, a corresponding small oscillation was induced in the wing.

It seemed most likely that the trimmer oscillation was the result of flow separation in the region of the flap, since the Reynoulds number (5×10^4) indicated laminar flow over the flap. Tho trimmer alone was then tested in a smaller tunnel (15" x 18" test section), to verify this assumption. Leading-edge grit and vortex generators attached to the trimmer seemed to have little if any effect on the trimmer oscillations, however, a spanwise rod held just above or below the trimmer surface completely eliminated the oscillations.

As a result of these tests, two new trimmers were constructed having flap chords of 20 and 30 percent of the trimmer chord. The intentions were to reduce the amount of control deflection required to trim the wing and thus prevent flow separation. When tested in the wind tunnel, however, the same characteristics were observed as for the original trimmer. It was later determined that the observed results were due to a block of wood attached to the tunnel floor to support the models. This block was not only allowing the transmisson of tunnel vibrations to the model, but disturbing the flow over the trimmer. With the elimination of these effects, the oscillation disappeared, and the results of trimmer angle-of-attack for control deflections shown in Figures 15 and 16 were obtained.

When testing was continued in the large tunnel, it was decided to investigate the effect of trimmer camber in the same direction and opposite to the wing camber direction, since the orientation was not clear from the investigation of Reference 3. Also at this time, future testing was limited to an investigation of four trimmer configurations only, these being the 20 and 30 percent flap chord trimmers pivoted at the 10 and 19 percent chord positions.

No significant difference in static response was observed due to camber direction, although dynamic response of the wing/trimmer system seemed to give the most promise for camber orientation in the same direction. The trimmer oscillation observed earlier in the test program, was again apparent for moderate flap deflections for all trimmer configurations. It also became clear that the wing trim angle was extremely sensitive to flap deflection.

Since it seemed critical to eliminate the trimmer oscillation problem before testing continued, a frame was constructed around the test section to which the model support wires were attached. This totally isolated the model from the tunnel wall vibrations other than those induced in the flowfield by the wind tunnel, however, no significant changes in the trimmer oscillation was observed.

The only remaining explanation of this oscillatory behavior was that the flow direction in the vicinity of the trimmer must be changing, thus causing the trimmer to oscillate seeking equilibrium. Due to the location of the trimmer, the most obvious factor to cause this is the upwash from the tip vortex of the wing. With the wing oscillating in its' stall region, the significant variation in lift and thus upwash velocity at the trimmer, would cause a change in effective angle-of -attack of the trimmer.

To verify this assumption, the wing and trimmer potentiometers were calibrated and connected to their respective surfaces in order to obtain the wing and trimmer angles-of-attack for various control deflections. At this point it was discovered that one single equilibrium position was difficult to establish, especially in the case of the trimmer, and the dynamic response of the system was not at all as anticipated. From these test results, it was concluded that the torque due to friction in the trimmer potentiometer was sufficiently large to affect the response of the trimmer and mask the aerodynamic trim position.

The trimmer potentiometer was disconnected for all succeeding tests, although the wing remained connected since its' angle-of-attack and response to a disturbance ia a critical parameter. With most of the friction in the trimmer thus eliminated, the wing was observed to have a change in angle-of-attack of 10 to 12 degrees resulting from a trimmer flap deflection of only 2 to 4 degrees, depending upon whether the trimmer was pivoted at the 19 or 10 percent chord position. While trimmer oscillation was not always accompanied by the wing operating in its' stall region, there was sufficient evidence to support the assumption of varying upwash on the trimmer.

There was still a tendency of the wing in some cases to return to a new equilibrium position after a disturbance. Since friction in the wing potentiometer was the likely cause of this, the potentiometer was replaced by a resolver, and the final few tests were conducted. As expected, much of this problem was eliminated, and the response of the wing improved.

RESULTS

Due to the extreme control sensitivity of the free-wing / free-trimmer model, there was considerable difficulty in obtaining more than a few data points for a comparitive study. Only two trim conditions could be obtained with any consistency and degree of reliability in the range of positive lift coefficients. These trim points were at wing angles-of-attack in the range of -1 to 1 degree and at about 10 degrees, corresponding to control deflections of 0 to 3 degrees, and a trimmer pivot location of ten percent of chord.

The wing seemed to be less sensitive to control deflection at these points, and once trim was established, the response was very similar in each test. The wing response for displacements to +10 and -15 degrees at these trim conditions are shown in Figure 10. The only difference noted was an inconsistency in the number of oscillations, which seemed to be the result of variations in the tunnel velocity due to temperature change in the fluid coupling drive system.

The conditions for which reliable responses were obtained are listed in Table 3. As indicated by this table, the amount of data obtained in this investigation was small, so an analysis of the dynamic response was not

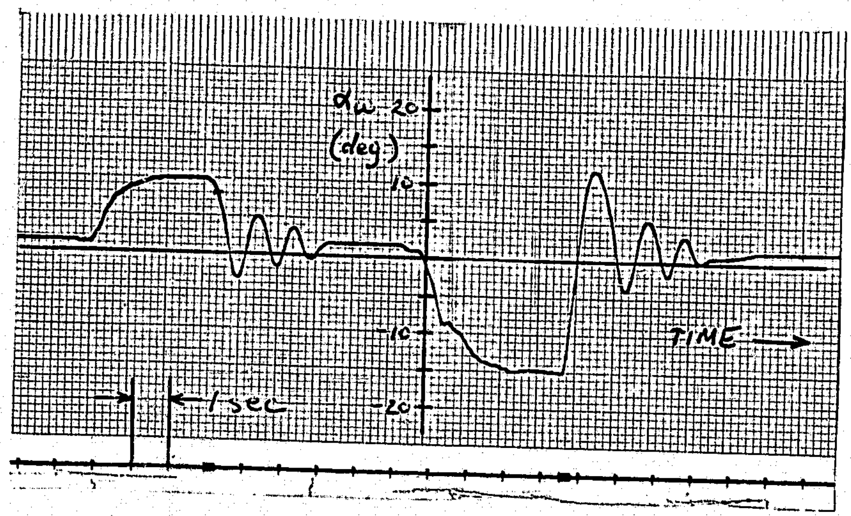

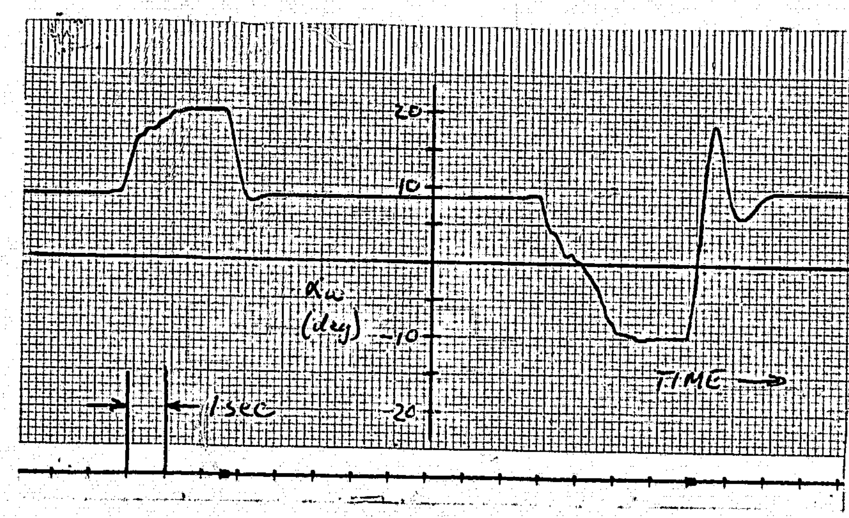

FIGURE 10: WING RESPONSE FOR DISPLACEMENTS FROM TWO INITIAL EQUILIBRIUM POSITIONS

attempted.

TABLE 3: INITIAL TRIM CONDITIONS OF THE TEST POINTS

Trimmer pivot location (% c)	Flap size c_f / c	Flap deflection (deg)	Wing angle of attack (deg)
10	.20	0	1
10	.20	0	1
10	.20	-2	-1
10	.20	-3	0
10	.20	1	1.5
10	.20	3	10
10 (small trimmer)	.20	0	0
10 (small trimmer)	.20	-2	-9
10 (small trimmer)	.20	3	-1
10 (reversed camber)	.20	0	-1
19	.20	-2	0
19	.20	0	13
19	.20	-1	2

Figure 11 shows a comparison of the oscillation patterns obtained for four different configurations with zero control deflection in all cases. It is seen that a similar oscillation exists for both the small and large trimmer surfaces when the wing and trimmer cambers have the same direction and the pivot is at the 10 percent

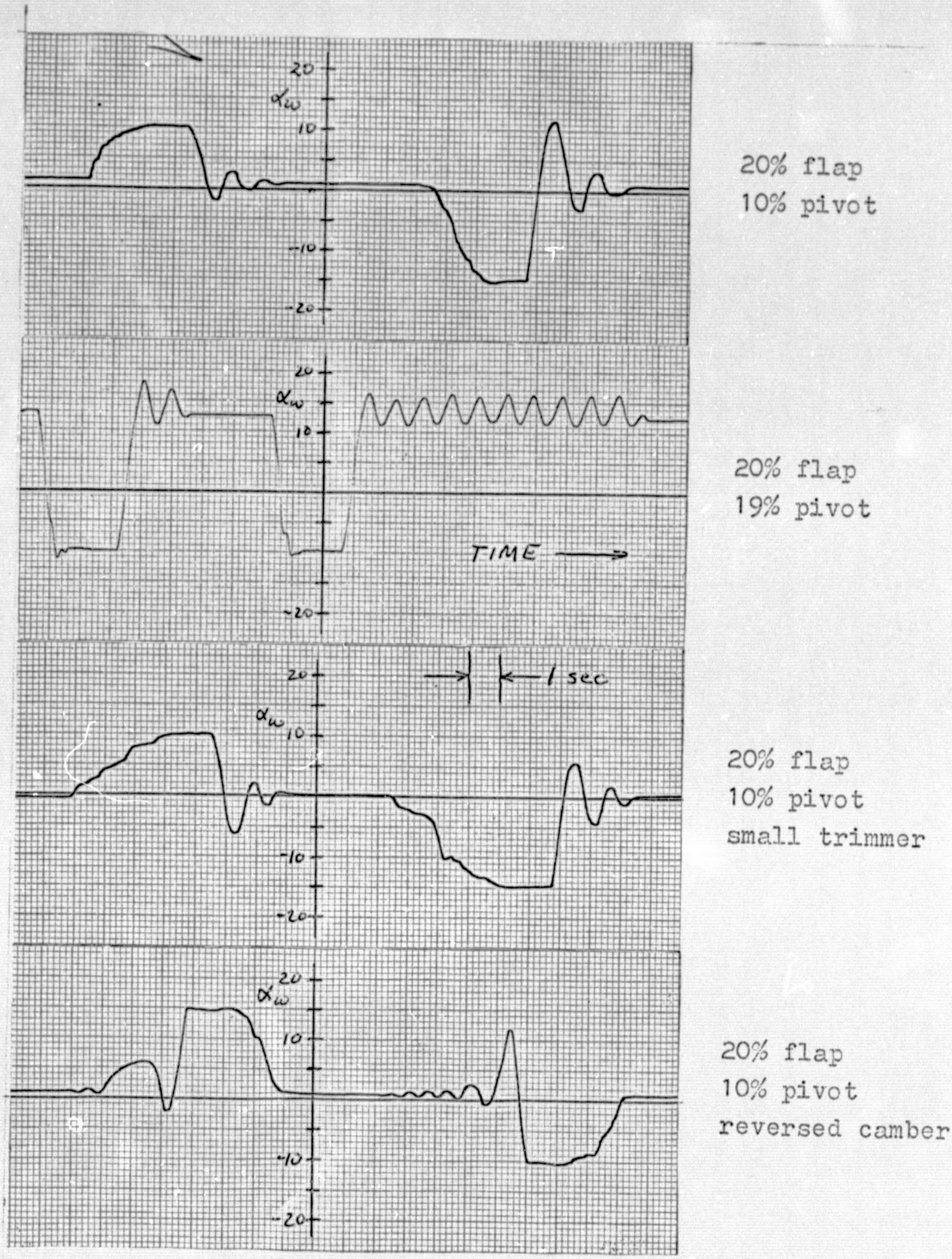

FIGURE 11: COMPARISON OF WING RESPONSE OF FOUR DIFFERENT CONFIGURATIONS WITH FLAP DEFLECTION OF ZERO

chord position. When the pivot is moved to the 19 percent position, the wing responds from a negative displacement by rotating to it's stall region where it is trapped in a constant amplitude oscillation. For the trimmer with a camber direction opposite to that of the wing, an unsatisfactory oscillation is seen to occur.

The response curves shown in Figures 10 and 11 were from the last few tests conducted in this investigation, in which the potentiometer had been replaced by a resolver. As an indication of the effects of potentiometer friction, Figure 12 is from a test run with both the trimmer and wing connected to their respective potentiometers. From an initial trim position of -6.5 degrees, the wing was displaced to 15 degrees positive and released. The effect of overdamping in the trimmer response due to friction is clearly indicated, while wing response is more as to be expected. When the system returned to equilibrium, both the wing and trimmer stabilized at new positions. Furthermore, when the wing was displaced to -10 degrees and released, there was no response of the trimmer, and again new equilibrium positions were established.

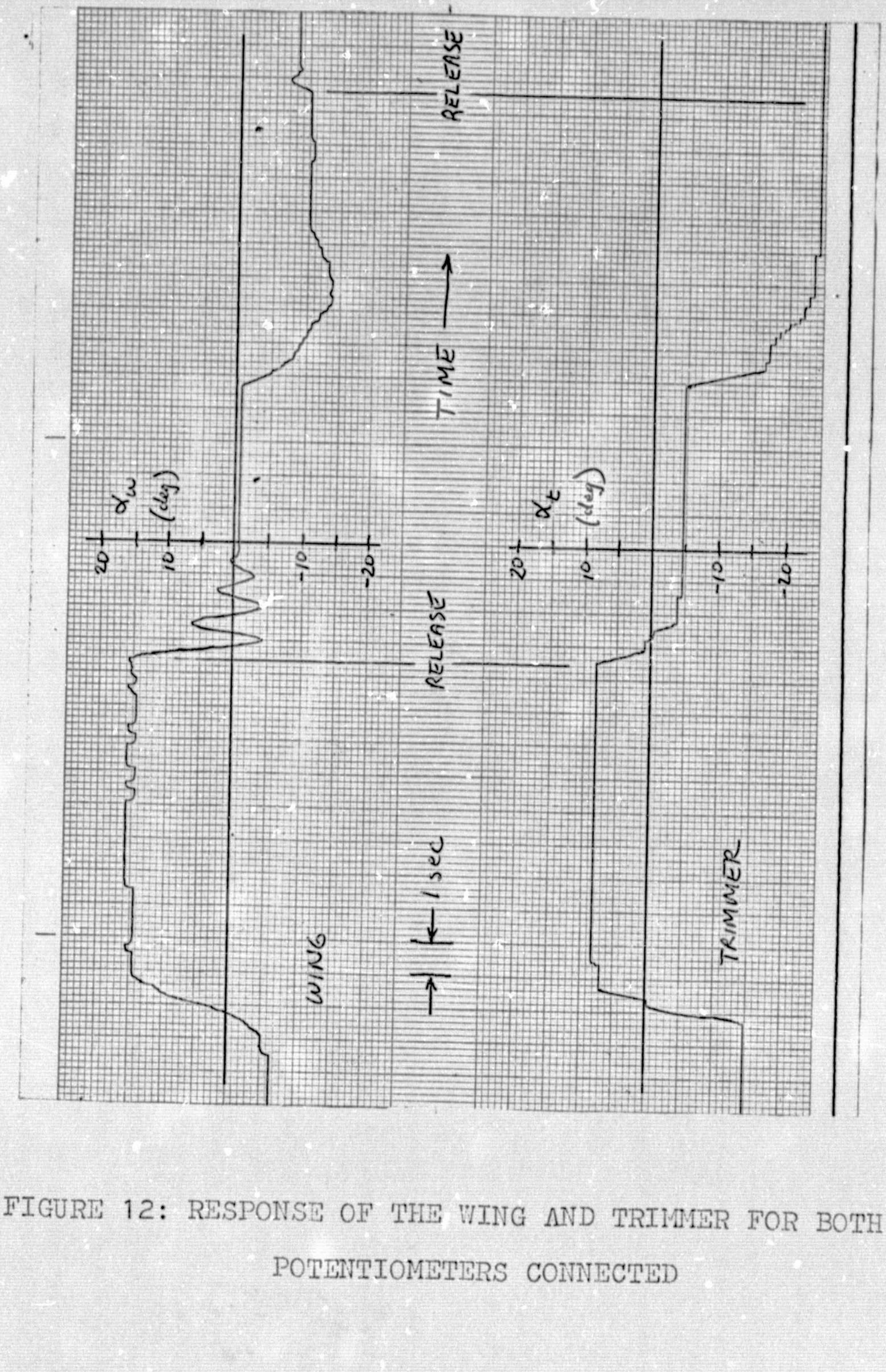

FIGURE 12: RESPONSE OF THE WING AND TRIMMER FOR BOTH POTENTIOMETERS CONNECTED

DISCUSSION

The largest problem encountered in this investigation was the magnitude of the frictional forces with respect to the aerodynamic moments. In particular, the friction in the trimmer potentiometer was determined to be as great as the aerodynamic moments associated with the trimmer, so little if no response was obtained.

The substitution of the resolver showed a definite improvement in wing response, and in future tests the relative magnitude of the friction should be reduced even more. The two ways of accomplishing this are to devise an alternate method of recording angular displacements, or to increase the aerodynamic moments of the wing and trimmer surfaces.

Unless an electrical recording scheme can be devised which has less friction than the resolver used in this investigation, it would appear that high-speed photography would be the best approach to eliminating friction. Unfortunately, this would be costly, and some of the wing and trimmer response would be lost.

The most practical approach to reducing the frictional effects is to increase either the model size or the tunnel flow velocity, resulting in an increase in the Reynolds number. It may be shown that the ratio of the aerodynamic moments about a pivot located a distance x from the aerodynamic center, to a constant frictional torque is;

$$\frac{M_p}{F} = \frac{1}{2} \nu^2 \rho \ AR \ (C_l \frac{x}{c} - C_m) \frac{c}{F} Rn^2$$

The variation of this ratio with Reynolds number is plotted in Figure 13 for parameter values representative of this study. As indicated by these curves, ratios of 5 and 23 to one could be obtained for the same trimmer and wing respectively, by an increase in tunnel velocity to 50 feet per second, and the use of resolvers on both surfaces. An added benefit of the increase in Reynolds number would be less tendency of flow seperation over the surface.

Another critical factor in obtaining consistant results in a free-wing / free-trimmer analysis is the control sensitivity. It was very difficult to measure the actual trimmer flap deflection, due to the limited range of travel corresponding to full wing deflection. As a result, most of the flap angles were estimated rather than measured. With a decrease in control sensitivity, a wider range of initial trim conditions could be established.

Defining the control sensitivity as the partial derivative of the wing angle-of-attack with respect to

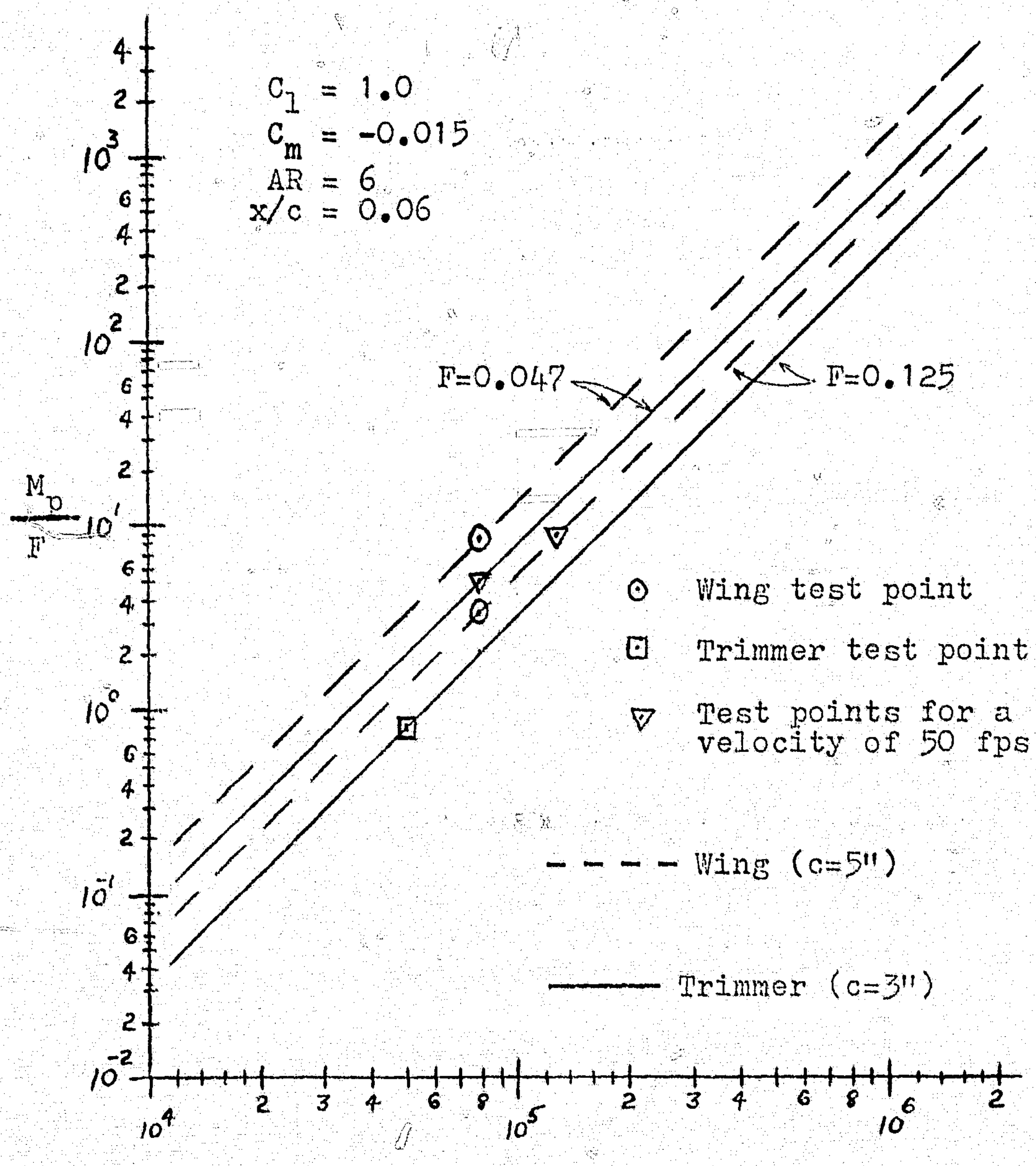

FIGURE 13 : MAGNITUDE OF THE AERODYNAMIC MOMENTS ASSOCIATED WITH REYNOLDS NUMBER

trimmer flap deflection, it's relationship to the model geometric parameters can be determined.

Referring to Figure 14, a moment balance about the wing and trimmer pivots gives;

$$C_l = \frac{c}{x}\left(C_m - \frac{S_t h}{S\, c} C_{l_t}\right) \qquad \text{(Equation 1)}$$

and

$$C_{l_t} = \frac{c_t}{x_t}\, C_{m_t}\Big|_{\delta} \qquad \text{(Equation 2)}$$

where $C_{m_t}\Big|_{\delta}$ is the pitching moment coefficient of the trimmer due to a flap deflection angle of δ. For a small range of flap deflection the change in the moment coefficient is approximately linear, therefore;

$$C_{m_t}\Big|_{\delta} = C_{m_t}\Big|_{\delta=0} + \delta\frac{\partial C_{m_t}}{\partial \delta} = C_{m_t} + \delta C_{m_{t\delta}}$$

and Equation 2 can be expressed as

$$C_{l_t} = \frac{c_t}{x_t}\left(C_{m_t} + \delta\, C_{m_{t\delta}}\right) \qquad \text{(Equation 3)}$$

With the further relation,

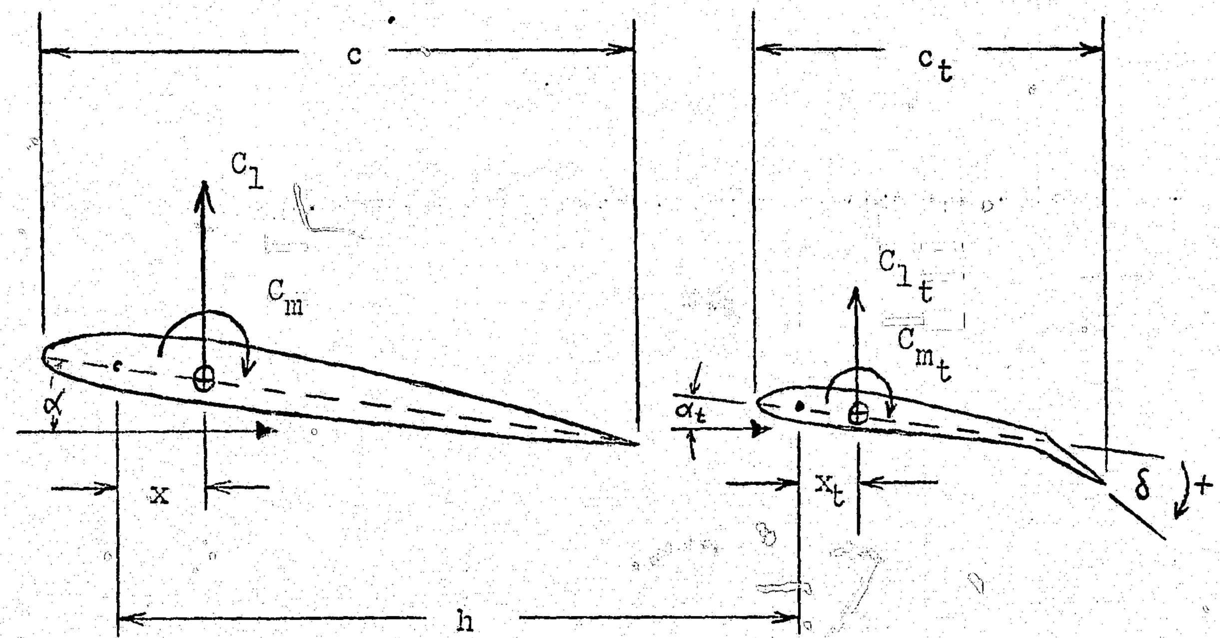

FIGURE 14: FREE-BODY DIAGRAM OF THE FREE-WING/FREE-TRIMMER CONFIGURATION

$$\alpha = \frac{C_l}{a} + \alpha_{l_0}$$

the angle-of-attack of the wing can be expressed in terms of control deflection as;

$$\alpha = \frac{c}{xa}\left(C_m - \frac{S_t}{S}\frac{h}{c}\frac{c_t}{x_t}\left(C_{m_t} + \delta\, C_{m_{t\delta}}\right)\right) + \alpha_{l_0} \quad \text{(Equation 4)}$$

The control sensitivity is therefore;

$$\frac{\partial\alpha}{\partial\delta} = -\frac{c}{xa}\,\frac{S_t}{S}\,\frac{h}{c}\,\frac{c_t}{x_t}\,C_{m_{t\delta}} \quad \text{(Equation 5)}$$

and since $C_{m_{t\delta}}$ is negative, the angle-of-attack of the wing changes positively for a positive flap deflection. Equation 5 indicates a linear relationship between the geometric parameters and the control sensitivity, and for this investigation the values were 2.5 and 6.2 degrees per degree for trimmer pivot locations of 10 and 19 percent of chord. The value of $C_{m_{t\delta}}$ was obtained from page 192 of Reference 4, and the slope-of-the-lift-curve was corrected for aspect ratio from the NACA 23012 airfoil data using the well-known relation;

$$a = \frac{a_0}{1 + \dfrac{57.3\, a_0}{\pi\, AR}}$$

It may be shown by a similar analysis, that the addition of a flap on the wing will have little, if no effect on the control sensitivity. Since it is also undesirable to decrease the trimmer-wing area ratio, due to a corresponding decrease in aerodynamic moments, the most practical means of reducing the control sensitivity, is to increase the pivot to aerodynamic center distance on both the wing and trimmer. A reduction in trimmer flap area will also result in less control effectiveness, since C_{m_t} is decreased. In Reference 5, a radio-controlled model employing the free-wing/free-trimmer concept was constructed and tested. To prevent an overly sensitive response, it was found necessary to pivot the wing at the 5 percent chord position, the trimmer at 13 percent, and to reduce the trimmer flap area by 50 percent.

A more foward pivot location would result in a more stable system, as the tests at the 10 and 19 percent pivot locations seemed to indicate. In many cases, trimmer oscillation was noticed at the 19 percent pivot, even for very small control deflections.

The tests conducted of the trimmer itself also indicated a slight oscillation at the 19 percent chord position, while the more foward pivot was very stable. These results are shown in Figure 15 and 16 along with the predicted results. Since the trimmer aspect ratio was very low, the slope-of -the-lift curve is estimated

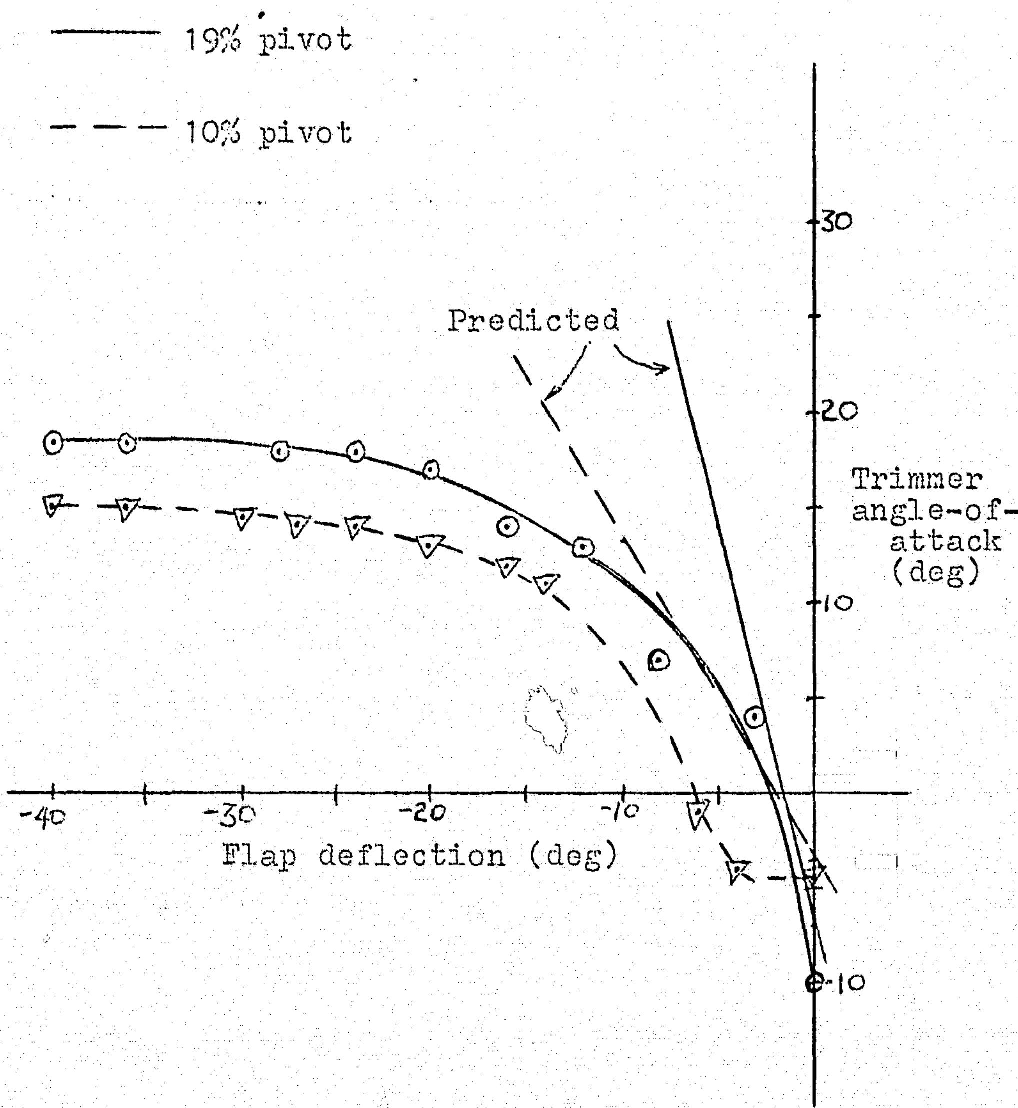

FIGURE 15: TRIMMER ANGLE-OF-ATTACK FOR FLAP DEFLECTION OF 20% CHORD FLAP

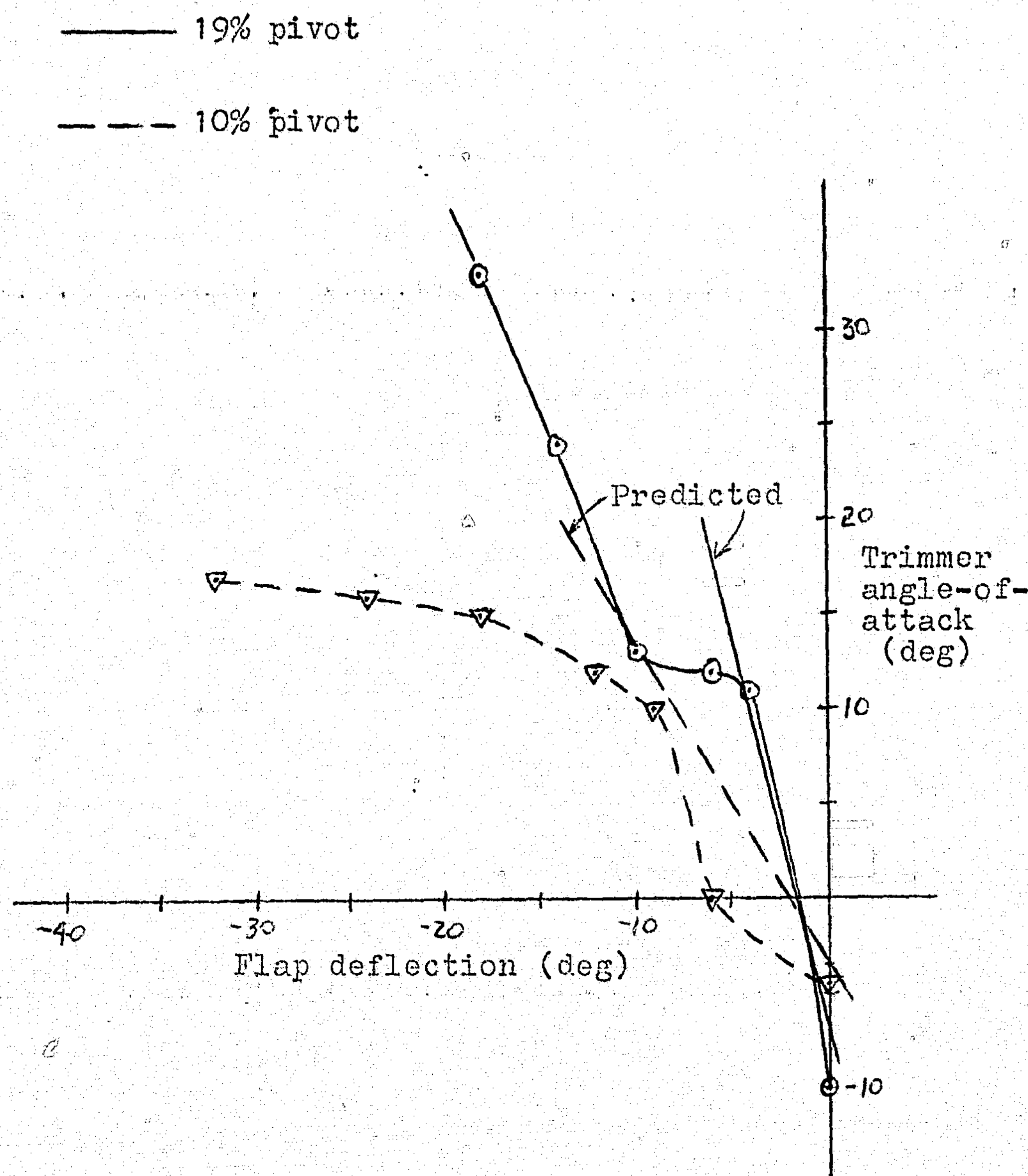

FIGURE 16: TRIMMER ANGLE-OF-ATTACK FOR FLAP DEFLECTION OF 30% CHORD FLAP

from Page 4 of Reference 6 as,

$$a_t = \frac{\pi\, AR_t}{1+\sqrt{1 + (\pi AR_t/a_o)^2}} \text{ , and}$$

the lift coefficient from Equation 3.

Insufficient test results were obtained for the wing/trimmer configuration with opposite camber directions, so a comparison cannot be made to the data obtained for the same orientation. However, the few tests that were run seemed to indicate that a better dynamic response resulted for cambers in the same direction, but more tests are need to verify this.

The wing trim angle for the conditions listed in Table 3 are shown plotted in Figure 17 along with the analytical results obtained from Equation 5. The wide scattering of the data points is to be expected due to the nature of the estimated control deflection angles, however they do tend to approximate the values shown by the lines.

As a final consideration, an estimate of the upwash velocity to be expected in the vicinity of the trimmer is computed. Since the trimmer establishes its' equilibrium positions according to the lift coefficient, the upwash is a factor only in determining the angle of displacement of the trimmer with respect to the wing and free stream direction. This effect is included here,

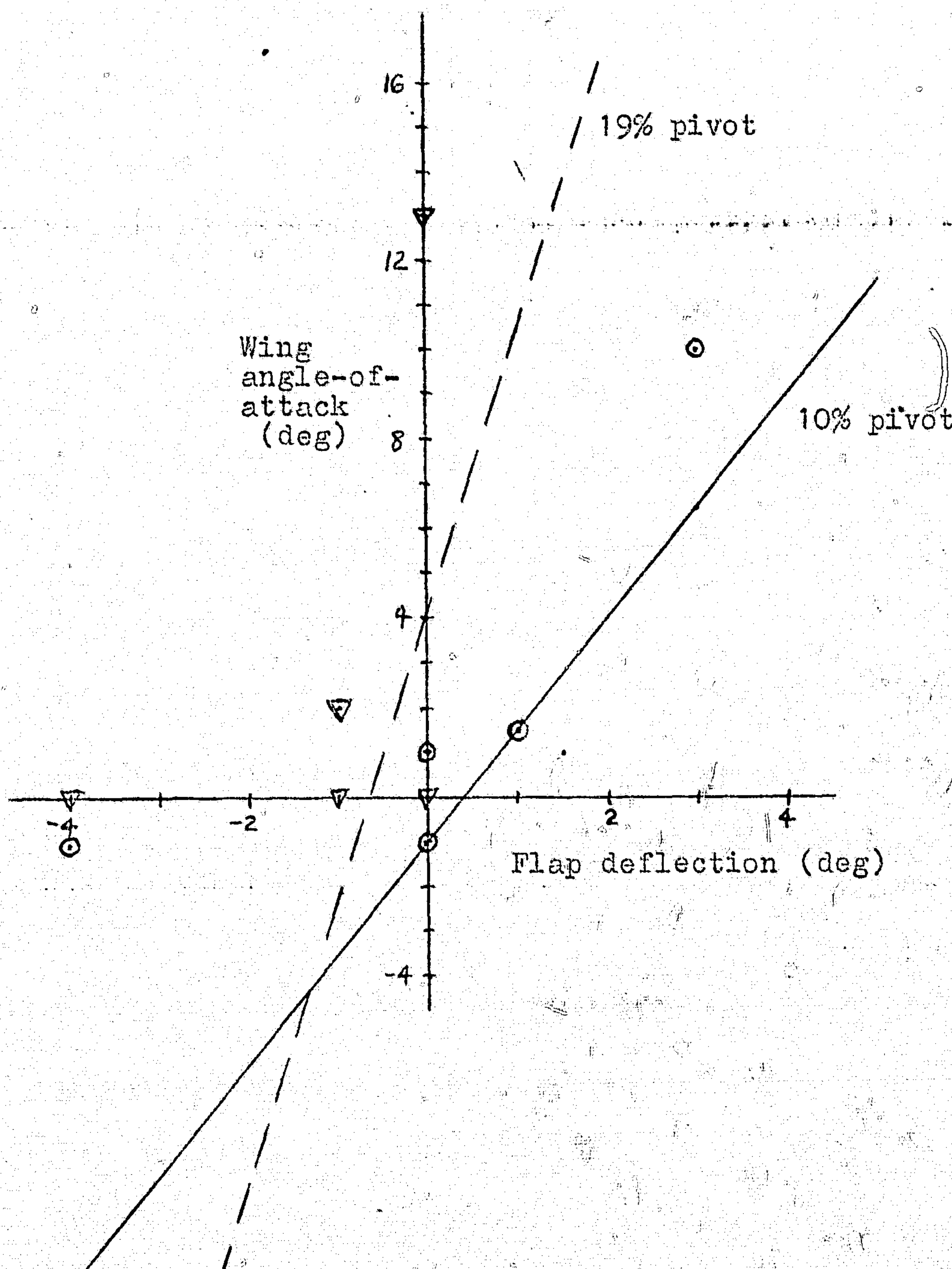

FIGURE 17: WING ANGLE-OF-ATTACK FOR VARIOUS FLAP DEFLECTIONS

however, for completeness.

By replacing the wing with a single horseshoe vortex, the circulation is constant, and from Page 157 of Reference 7, equal to;

$$\Gamma = \frac{VSC_l}{2b}$$

Since a semi-span wing is being analyzed, only half of the horseshoe vortex is considered. Neglecting the contribution of the bound vortex, the upwash at a point due to the trailing vortex is;

$$\omega = \frac{\Gamma}{4\pi h}(\cos\alpha + \cos\beta) \qquad \text{(Equation 6)}$$

where h is the perpendicular distance from the vortex core to the point being considered, and α and β are the angles between a line from the point to the ends of the vortex and the vortex filament. If x is the distance aft to the point from the bound vortex, Equation 6 becomes,

$$\omega = \frac{\Gamma}{4\pi h}\left[1 + \frac{x}{\sqrt{x^2+h^2}}\right]$$

$$= \frac{VSC_l}{8\pi h}\left[\frac{1}{h} + \frac{x}{\sqrt{x^2+h^2}}\right]$$

Figure 18 shows the variation in upwash across the

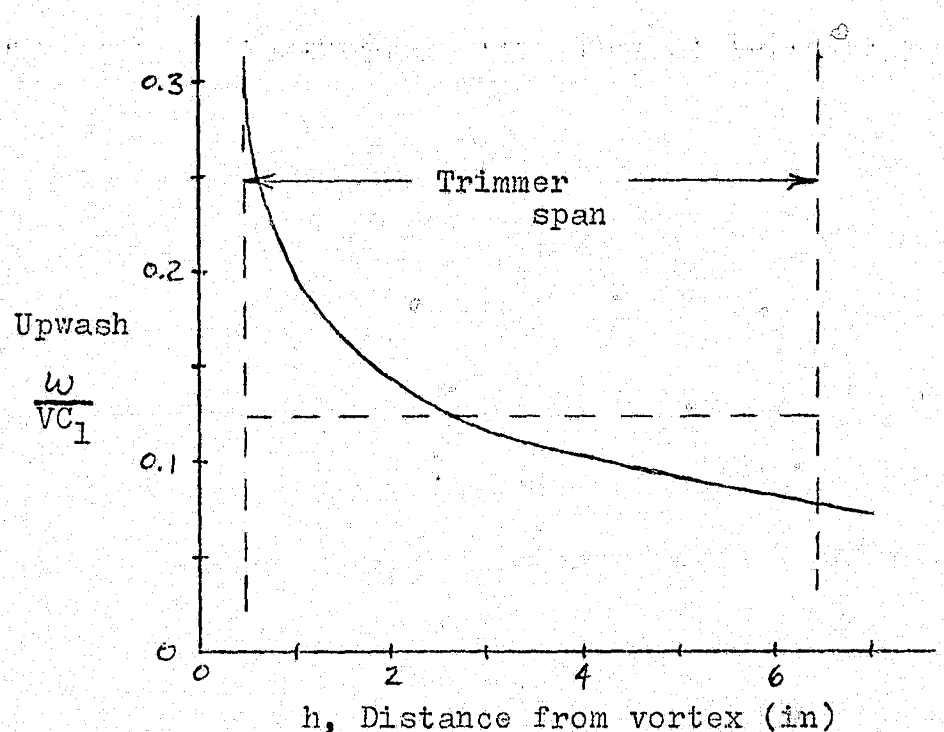

FIGURE 18: UPWASH ALONG TRIMMER SURFACE

trimmer for the model tested in this investigation.

RECOMMENDATIONS

From the results of this investigation, the following recommendations for future wind tunnel testing are presented:

(1) The ratio of aerodynamic moments to frictional torque must be as high as possible. The easiest way of doing this is by increasing the chord of the test model and/or increasing the flow velocity

(2) The control sensitivity must be adjusted to give a greater range of flap deflection for the same change in wing angle-of-attack, thus making it easier to determine flap deflection and obtain a wider range of trim conditions. This can be accomplished by moving the wing pivot foward.

(3) Further testing is needed to determine the optimum direction of trimmer camber.

(4) A flap should be added to the wing to determine the maximum lift coefficient that can be obtained for changes in pivot position and distance between the wing and trimmer pivot points.

(5) If angular changes are to be measured electrically, a resolver should be used, and the results verified by limited high-speed photography

REFERENCES

(1) Porter, R.F. and Brown, J.H., Jr., "Evaluation of the Gust-Alleviation Characteristics and Handling Qualities of a Free-Wing Aircraft", NASA CR-1523, April 1970.

(2) Porter, R.F., Luce, R.G. and Brown, J.H., Jr., "Investigation of the Applicability of the Free-Wing Principle to light General Aircraft", NASA CR-2046 June 1972.

(3) Porter, R.F., Hall, D.W., Brown, J.H., Jr., and Gregorek, G.M., "Analytical Study of a Free-Wing/Free-Trimmer Concept", NASA CR-2946, 1978.

(4) Abbott, Ira H., and von Doenhoff, Albert E; <u>Theory of Wing Sections</u>, Dover Publications, Inc., New York, 1959.

(5) Gee, Shu W. and Brown, Samuel R., "Flight Tests of a Radio Controlled Airplane Model With a Free-Wing/Free-Canard Configuration", NASA TM-72853, March 1978.

(6) Seckel, Edward ; <u>Stability and Control of Airplanes and Helicopters</u>, Academic Press, New York, 1964.

(7) Dommasch, Daniel O., Sherby, Sydney S., and Connolly, Thomas F. ; <u>Airplane Aerodynamics</u>, Pitman Publishing Company, New York, 4 th Edition, 1967.

BIBLIOGRAPHY

(1) Babister; "Aircraft Stability and Control", Volume 1, International Series of Monographs in Aeronautics and Astronautics, Pergamon Press, London, 1961.

(2) Clancy, J.L.; Aerodynamics , Wiley and Sons,New York, 1975.

(3) Etkin,B. ; Dynamics of Flight, Stability and Control, Wiley and Sons, New York, 1959.

(4) Pierce, H.B., "Investigation of the Dynamic Response of Airplane Wings to Gusts", NACA TN 1320, June 1947.